HHS Public Access

Author manuscript

J Immunol. Author manuscript; available in PMC 2021 November 15.

Published in final edited form as:

J Immunol. 2020 November 15; 205(10): 2786–2794. doi:10.4049/jimmunol.2000784.

Non-cell-autonomous activity of the hemidesmosomal protein BP180/collagen XVII in granulopoiesis in humanized NC16A mice

Lin Lin[#a,b], **Bin-Jin Hwang**[#a,c], **Ning Li**[a], **Paul Googe**[a], **Luis A. Diaz**[a], **Ed. Miao**[c], **Barbara Vilen**[c], **Nancy E. Thomas**[a], **Jenny Ting**[d], **Zhi Liu**[a,c]

[a.]Department of Dermatology, University of North Carolina, Chapel Hill, NC

[b.]Oral Biology Program, School of Dentistry, University of North Carolina, Chapel Hill, NC

[c.]Department of Microbiology and Immunology, University of North Carolina, Chapel Hill, NC

[d.]Department of Genetics, University of North Carolina, Chapel Hill, NC

[#] These authors contributed equally to this work.

Abstract

BP180 (also termed type XVII collagen) is a hemidesmosomal protein and plays a critical role in cell-cell matrix adhesion in the skin; however, its other biological functions are largely unclear. Here, we generated a BP180 functional deficient mouse strain by deleting its extracellular domain of humanized NC16A (termed *ΔNC16A* mice). We found that BP180 is expressed by bone marrow mesenchymal stem cells (BM-MSC) and its functional deficiency leads to myeloid hyperplasia. Altered granulopoiesis in *ΔNC16A* mice is through bone marrow stromal cells evidenced by bone marrow transplantation. Furthermore, the level of G-CSF in bone marrow and circulation were significantly increased in *ΔNC16A* mice as compared to WT mice. The increased G-CSF was accompanied by an increased activation of the NF-κB signaling pathway in bone marrow and BM-MSC of *ΔNC16A* mice. Blockade of G-CSF restored normal granulopoiesis in *ΔNC16A* mice. Inhibition of NF-κB signaling pathway significantly reduces the release of G-CSF from *ΔNC16A* bone-marrow mesenchymal stem cells in vitro and the level of serum G-CSF in *ΔNC16A* mice. These findings provide the first direct evidence that BP180 plays an important role in granulopoiesis through regulating NF-κB signaling pathway in BM-MSC.

Keywords

BP180/ Collagen XVII; hemidesmosome; granulopoiesis; NF-κB; G-CSF

Corresponding author: **Zhi Liu**, PhD, Department of Dermatology, University of North Carolina at Chapel Hill, 2360 Genome Sciences Building, CB#7287, Chapel Hill, North Carolina 27599, USA. zhi_liu@med.unc.edu Phone: 919-966-0788, Fax: 919-966-3898.

The current affiliation of BJ. Hwang is Department of Surgery, School of Medicine, Duke University, NC, USA.

The current affiliation of Ed Miao is Department of Immunology, School of Medicine, Duke University, NC, USA.

Introduction

BP180 (also termed type XVII collagen) is a 180-kDa transmembrane hemidesmosomal protein (1). The intracellular region of BP180 is linked to the intermediate filament network and its extracellular portion is anchored into the basement membrane zone (BMZ) through interaction with extracellular matrix proteins (2)(3)(4). BP180 as a critical cell-cell matrix adhesion protein was illustrated by two human subepidermal blistering diseases; Bullous Pemphigoid (BP) caused by anti-BP180 autoantibodies that attack and impair function of BP180 autoantigen in basal keratinocytes (5)(6) and Generalized Atrophic Benign Epidermolysis Bullosa (GABEB, a type of junctional epidermolysis bullosa, JEB) caused by BP180 gene mutations (7)(8)(9). However, whether BP180 is involved in other biological processes and pathological conditions is largely unknown.

BP is the most common skin autoimmune blistering disease characterized by autoantibodies directed against the hemidesmosomal proteins BP230 and BP180, dermal-epidermal junction separation and inflammatory cell infiltration (10). Patients with BP have eosinophils and neutrophils in the bullous cavity and dermis of the lesioned skin (1). The membrane-proximal non-collagen 16A (NC16A) linker domain harbors multiple epitopes recognized by BP autoantibodies (11)(12). Although human BP180 shares high overall homology with mouse BP180, the NC16A domain is very poorly conserved with the counterpart of mouse BP180 (termed NC14A), resulting in a lack of immune cross-reactivity between these two species (6). Animal models of BP demonstrated that anti-NC14A and anti-NC16A antibodies induce subepidermal blistering in mice associated with neutrophil infiltration (6)(13).

Junctional epidermolysis bullosa (JEB) is a group of rare genetic diseases characterized by marked skin fragility and blister formation following minor trauma, along with eosinophilia, eosinophils and/or neutrophils infiltration in the dermis (14).

BP180 mutations lead to the partial or complete loss of BP180 function, causing JEB, which is commonly termed as non-Herlitz JEB (15)(16). Patients with non-Herlitz JEB exhibited a wide spectrum of clinical outcomes, from mild to severe phenotypes of JEB symptoms (17). In general, the milder forms of JEB are associated with missense or splice-site mutations and the presence of truncated BP180 protein in the skin (17)(18)(19). Previous reports demonstrated that deletion of NC14A domain of mouse BP180 leads to loss of cell-cell matrix adhesion and granulocyte infiltration in the skin (20). However, the mechanisms underlying the increased granulocytes in BP/JEB patients and mice lacking BP180 function are unknown.

Multipotent hematopoietic stem cells undergo intermediate development stages, giving rise to a $lin^{-}IL7R^{-}KIT^{+}Sca\text{-}1^{-}CD34^{+}FcrR^{lo}$ common myeloid progenitor (CMP), and CMPs then differentiate into megakaryocyte/erythrocyte and granulocyte/macrophage progenitors (GMP) (21)(22)(23)(24). Neutrophils, eosinophils and basophils constitute the three main types of granulocytes. Large quantities of neutrophils are produced and stored in the bone marrow (25)(26). Granulopoiesis is regulated by cell-autonomous and non-cell-autonomous mechanisms (27)(28). G-CSF is a major determinant of non-cell-autonomous mechanism in

granulocyte differentiation, proliferation and maturation (27)(29)(30). G-CSF is also important for neutrophil mobilization (31). G-CSF is secreted by bone marrow stromal cells, endothelial cells, macrophages and fibroblast cells (32). Deficiency of G-CSF or G-CSF receptor causes neutropenia in mice, and administration of G-CSF is a clinical practice to treat neutropenia (33), demonstrating that G-CSF is an important extrinsic regulator for neutrophils (32)(34).

Homeostasis of hematopoietic stem cells (HSCs) in bone marrow is dependent on multiple signaling pathways (35)(36), including Notch and NF-κB as two of the most investigated signaling pathways (37)(38). The bone marrow niche regulates hematopoiesis in a NF-κB dependent manner (39)(40)(41). NF-κB is a protein complex composed of inhibitory component IκBα and DNA binding p65/39. Upon external signal stimulations, NF-κB is phosphorylated. As a result, phosphorylated IκBα is degraded and phosphorylated p65 is transported to nucleus to activate the transcription of its downstream genes (42), including the gene encoding G-CSF(43). Loss of transcriptional repression of NF-κB activation in IκBα-deficient mice leads to an uncontrolled expansion of myeloid cells via G-CSF (44) (45).

In this study, we used mouse strains lacking BP180 function by deleting the humanized NC16A domain of the molecule to investigate new functions of BP180 (46). We show that deletion of the BP180 NC16A domain leads to altered granulopoiesis. To our knowledge, this is the first report linking BP180 in bone marrow stromal cells and granulopoiesis.

Material and Methods

In vivo mouse models and bone marrow transplantation

Humanized NC16A and *ΔNC16A* mice were described previously (13)(46). Briefly, mouse NC14A-encoding exons were replaced by human NC16A-encoding exons flanked by loxP sites. This approach offers one step transgenic manipulation to produce both humanized NC16A mice and conditional NC16A-deletion mice. NC16A mice were then bred with germline Cre mice (The Jackson Laboratory, Maine, USA) (both on C57BL/6J background), leading to removal of NC16A-encoding exons and expression of NC16A-truncated BP180 in *ΔNC16A mice* (46). Mice with skin-specific deletion of NC16A were generated by crossing NC16A mice with K14Cre mice (46). C57BL/6 (CD45.1 and CD45.2) mice were purchased from National Cancer Institute. To make mixed bone marrow chimera, bone marrow from *ΔNC16A* CD45.2 and WT CD45.1 mice were mixed at 1:1 ratio, and then 5×10^6 cells were transplanted to sub-lethal irradiated (700 cGy) WT CD45.1.2 recipient mice by I.V. administration (47)(48).

All the mice were bred and hosted under specific pathogen-free conditions in the animal facilities of the University of North Carolina, Chapel Hill (UNC-CH). Animal care and animal experiments were conducted in accordance with the Animal Care Committee at UNC-CH.

Bone marrow derived-mesenchymal stem cells culture

Bone marrow cell isolation and culture were as described (49)(50). Briefly, bone marrow cell suspensions were isolated from 8–12 weeks ΔNC16A and WT control mice by flushing the marrow from femurs a few times with 10 ml PBS/2%FBS in syringe with a 22-G needle. The cells were centrifuged for 5 min at 1000 rpm, 4°c after red blood cells were lysed and removed. Cells were counted and seeded with MSC culture medium (MesenCult™ MSC culture medium, stem cell technologies, Vancouver, Canada) according to the protocol provided by the manufacture. Only the adherent monolayer cells were used as MSC after 2 washes with PBS to remove all non-adherent cells.

CFU assay

The colony forming capacity of bone marrow cells was estimated in mouse methylcellulose complete media containing mouse IL3, IL6, SCF, and human insulin, according to the manufacturer's instructions (Mouse Methylcellulose Complete Media without Epo, R&D Systems Inc. MN). (51). Briefly, 3×10^4 bone marrow mononuclear cells were mixed well in 1 ml media, plated in 3 cm diameter culture dishes, and then incubated at 37°C in a 5% CO_2 incubator. At nine days after plating, the total number of colonies in each dish was counted under a microscopy.

Flow cytometry

Bone marrow, spleen, lymph nodes and peripheral blood were taken from mice. 5×10^6 cells were used for staining. Bone marrow single cell suspension were made by flushing femurs a few times by 22 G needle and 10 ml syringe with 10 ml PBS/2%FBS. Spleen and lymph nodes were mashed by slides carefully and then passing through 70 μm cell strainer (FALCON, Corning, NY) to isolate single cell suspension. All cell suspensions were treated with ACK buffer for red blood cell lysis. 5×10^6 cells were used for staining. Anti-Gr-1 and anti-CD11b antibodies were used to detect granulocytes. Anti-CD3 antibody was used to detect T cells. Anti-CD19 antibody was used to detect B cells. Anti-CD127, CD34, CD16, Sca-1 and c-Kit antibodies were used to identify different population of granulocyte progenitors (Figure 3A). These antibodies were purchased from Biolegend (San Diego, CA).

Immunoblotting and immunofluorescence

Expression of BP180 in different tissues was determined by immunoblotting and immunofluorescence using standard techniques as previously described (13). The anti-NC16A antibody was from BP patient serum, while rabbit anti-NC1–3 polyclonal antibody was made in house. Femurs were fixed in 4% paraformaldehyde overnight and then decalcification by 14%EDTA overnight and then tissue was rinsed by PBS 3 times. The femurs were fixed in OCT (Tissue-TEK®, CA, USA). Cryosections of the OCT-embedded femurs were stained and were imaged by a Zeiss LSM 700 Confocal Laser Scanning Microscope and ZEN imaging software. The pictures were analyzed by Image-J software. Bone marrow cells and bone marrow derived mesenchymal stem cell (1×10^6) were used for NF-κB signaling pathway determination. After Pierce®BCA protein assay (Thermo Fisher Scientific), proteins were probed by the following antibodies: anti-Phospho ErK, anti-ErK,

anti-IκBα, anti-phospho-IκBα, anti-p65, anti-phospho p65 and anti-rabbit secondary antibody (Cell Signaling Technology®, MA, USA).

Quantification of G-CSF, GM-CSF by ELISA

Levels of G-CSF and GM-CSF in bone marrow supernatant and serum samples from *ΔNC16A*, K14Cre/*ΔNC16A* and WT control mice were quantified by ELISA kits (Abcam, MA, USA). ELISA Max™ Mouse GM-CSF ELISA kits were purchased from Biolegend. To collect bone marrow supernatants, marrows from femurs were flushed out with PBS and centrifuged. Collected supernatants were stored in −80°C before use.

Statistical analysis

The data are expressed as mean ± SEM and were analyzed using the Student's t-test. A p value less than 0.05 was considered significant.

Results

Δ*NC16A* mice have increased granulocyte-macrophage progenitors

Previously, we generated humanized NC16A mice to investigate pathogenesis of BP and *ΔNC16A* mice for studying the role of BP180 in skin inflammation (13)(46). *ΔNC16A* mice showed no clinical skin phenotypes after birth but began to develop minor skin lesions at the age of 8–12 weeks and erosions mostly on snout and ears after 16 weeks old (Supplemental Figure 1A). *ΔNC16A* mice also showed retarded growth (Supplemental Figure 1B). Genotyping of mouse tail DNA confirmed the lack of exons 18 and 19 in *ΔNC16A* mice (data not shown). Interestingly, necropsy on 8–12 weeks old *ΔNC16A* mice revealed splenomegaly and bone marrow color change from pink to gray in *ΔNC16A* mice (Figure 1A). Spleen/body weight ratio was significantly increased in *ΔNC16A* compared to WT control mice (Supplemental Figure 1C).

To explain these gross alterations in spleen and bone marrow, we analyzed the hematopoiesis system of *ΔNC16A* mice by routine histology, hematological examination, and flow cytometry. Histological examination showed increased granulocytes in blood and dermis, increased cellularity in bone marrow, and increased red pulp in spleen of *ΔNC16A* mice as compared to WT control (Figure1B). Hematological test showed significantly increased total cell number (Figure1C) and percentage (Figure1D) of granulocytes in circulation in *ΔNC16A* compared to WT mice. Normal granulocyte number range of WT mice is less than 20 percentage in white blood cells (41), while *ΔNC16A* mice manifested an abnormally high percentage of granulocytes in white blood cells in the peripheral blood. Flow cytometry analysis also showed significantly increased granulocytes in bone marrow, spleen and peripheral blood in *ΔNC16A* mice as compared to WT controls using forward scatter (cell size) and side scatter (granularity) (Figure1E) and granulocyte number counts based on the surface markers CD11b and Gr-1 (Figure1F). These results demonstrated that a lack of BP180 function caused myeloid hyperplasia.

In bone marrow hematopoietic stem cells are first differentiated into common myeloid progenitor and granulocyte monocyte progenitor (GMP), and then through various

developmental stages, eventually differentiated to neutrophils, basophils and eosinophils (Figure 2A)(42)(52)(53). Since there is granulocyte hyperplasia in *ΔNC16A* mice, we determined whether the progenitors of granulocytes in bone marrow of *ΔNC16A* mice were changed by flow cytometry using $Lin^{-}IL\text{-}7R^{-}SCA\text{-}1^{-}c\text{-}kit^{+}CD34^{+}$ $CD16^{+}$ surface markers combination panel (Figure 2A)(43)(44). We found that there was more than a two fold increase in GMP population in *ΔNC16A* mice compared to WT control (Figure 2B), which was statistically significant (Figure 2C). We also observed a significantly higher number of colony-forming units of granulocytes/monocytes from *ΔNC16A* bone marrow than WT control mice (Figure 2D). The hemoglobin content and platelet counts were not significantly different between WT and *ΔNC16A* mice (Supplemental Figure 2A and 2B). These results demonstrate that a lack of BP180 leads to myeloid progenitor lineage skewing toward GMPs, resulting in increased granulocyte production.

Granulopoiesis defects in Δ*NC16A* mice arise from non-cell-autonomous mechanism

Knowing that *ΔNC16A* mice develop granulocyte hyperplasia, we then determined if a cell-autonomous or non-cell-autonomous mechanism causes the significantly elevated granulocytes by bone marrow chimera and bone marrow transplantation experiments. Taking advantage of congenic marker, bone marrows of CD45.1 WT mice and CD45.2 *ΔNC16A* mice were mixed at 1:1 ratio and transferred to sub-lethally irradiated WT CD45.1.2 recipients (Figure 3A). After 8 weeks reconstitution, there was no difference between granulocyte populations derived from WT and *ΔNC16A* mice in bone marrow and spleen of host animals (Figure 3B). $Gr\text{-}1^{+}$ cell populations in bone marrow, spleen and lymph node were also comparable (Figure 3C). By bone marrow transplantation experiments, WT mice transplanted with WT or *ΔNC16A* bone marrow showed normal granulopoiesis, whereas *ΔNC16A* mice transplanted with WT or *ΔNC16A* bone marrow developed granulocyte hyperplasia similar to *ΔNC16A* mice (Figure 3D). These data suggested that altered granulocyte development in *ΔNC16A* mice is not caused by the defect in bone marrow cells themselves, but rather is caused by the dysfunction of BP180 in the radiation resistant compartment, the mesenchymal stem cells (MSC).

To sustain this possibility, we determined whether BP180 is expressed in bone marrow and/or MSC. Using immunoblotting, anti-NC16A antibody detected the full-length BP180 in whole bone marrow protein extract of WT and not *ΔNC16A* mice, whereas anti-NC1–3 antibody recognized both full-length and NC16A truncated BP180 in bone marrow of both WT and *ΔNC16A* mice (Figure 3E). By indirect immunofluorescence, anti-NC16A antibody stained bone marrow cryosection from WT, but not from *ΔNC16A* mice (Figure 3F). More importantly, BP180 expression was only detected in cultured bone marrow derived MSC but not in purified granulocytes and lymphocytes (Figure 3G). Taken together, these results showed that altered granulopoiesis *ΔNC16A* mice is due to BP180 functional deficiency in bone marrow stromal cells instead of a cell autonomous mechanism.

Δ*NC16A* mice exhibit elevated G-CSF levels and increased activation of NF-κB signaling pathway in bone marrow mesenchymal stem cells

Since G-CSF is a key regulator for granulopoiesis of non-cell autonomous mechanism and myeloid cell proliferation (25)(45), we used ELISA to quantify G-CSF expression levels

both in bone marrow supernatant and serum from *ΔNC16A* and WT mice. *ΔNC16A* mice had significantly higher G-CSF levels in bone marrow and serum compared to WT mice (Figure 4A, 4B). As a control, levels of GM-CSF in bone marrow and serum in *ΔNC16A* and WT mice were comparable (Figure 4C, 4D). To determine whether activation of NF-κB pathway was also increased in *ΔNC16A* mice as a potential molecular mechanism underlying the increased G-CSF expression and altered granulopoiesis, we examined whether NF-κB signaling is upregulated in the bone marrow of *ΔNC16A* mice. Immunoblotting results showed increased level of phosphorylated IκBα in the total bone marrow cells of *ΔNC16A* mice as compared to WT (Figure 4E and 4F).

To further confirm these findings, cultured bone marrow MSCs were assayed for activation of the NF-κB signaling pathway and release of G-CSF. Cultured bone marrow MSC from *ΔNC16A* mice showed significant increase of NF-κB signaling pathway (Figure 4G) and released significantly higher level of G-CSF than WT mice (Figure 4H). In contrast, there is no significant change in GM-CSF release between *ΔNC16A* and WT MSCs (Figure 4I). These results suggest that increased activation of NF-κB signaling pathway and release of G-CSF in bone marrow MSC contribute to the altered granulopoiesis and subsequently to elevated granulocytes in bone marrow, spleen, and peripheral blood in *ΔNC16A* mice.

Granulopoiesis in basal keratinocyte-specific Δ*NC16A* mice is normal

ΔNC16A mice start showing skin lesions at 8 weeks old. To rule out the possibility that altered granulopoiesis in *ΔNC16A* mice is secondary to skin lesion and inflammation, we crossed loxP floxed NC16A mice with K14Cre mice to generate mice with basal keratinocyte-specific deletion of NC16A (termed K14Cre/*ΔNC16A*)(46). As expected, K14Cre/*ΔNC16A* mice showed NC16A truncated BP180 in the skin and full-length BP180 in bone marrow as evidenced by immunoblotting (Figure 5A). Similar to *ΔNC16A* mice, K14Cre/*ΔNC16A* mice developed skin lesion starting at 8 weeks of age, including skin erosion and infiltration of CD3 positive T cell and Gr-1 positive granulocytes (Supplemental Figure 3)(46). By hematological examination, granulocyte numbers in peripheral blood of K14Cre/*ΔNC16A* mice were similar to WT mice but significantly lower than *ΔNC16A* mice (Figure 5B). By flow cytometry the granulocyte populations in bone marrow, spleen and blood in K14Cre/*ΔNC16A* mice were comparable to WT mice (Figure 5C). Furthermore, levels of G-CSF and GM-CSF in the serum of K14Cre/*ΔNC16A* mice were similar to WT mice, but G-CSF level of K14Cre/*ΔNC16A* mice were significantly lower than *ΔNC16A* mice (Figure 5D, 5E). These results indicate that loss of BP180 function in basal keratinocytes is not the cause of the altered granulopoiesis, further supporting that altered granulopoiesis in *ΔNC16A* mice is due to lack of BP180 function in bone marrow MSCs.

Δ*NC16A* mice at 4 weeks old show no skin lesion and exhibit abnormal granulopoiesis

To further confirm that altered granulopoiesis in *ΔNC16A* mice originates from bone marrow stromal cells, not skin lesion, we examined 4 weeks old *ΔNC16A* mice when clinical skin lesions are absent. Gross examination showed that 4 weeks old *ΔNC16A* mice do not exhibit skin abnormalities (Supplemental Figure 4A). Histological examination showed no skin inflammation including a lack of CD3 positive T cell and granulocyte infiltration in 4-week-old *ΔNC16A* mice (Supplemental Figure 4A). Similar to 8-week-old

ΔNC16A mice, however, 4-week-old *ΔNC16A* mice also had significantly increased granulocyte numbers in peripheral blood in comparison to WT mice, as determined by hematological examination (Supplemental Figure 4B). In addition, 4-week-old *ΔNC16A* mice had more granulocytes in bone marrow and blood but not in the spleen or blood when compared to WT mice as determined by flow cytometry using forward scatter, side scatter, Gr-1 and CD11b markers (Supplemental Figure 4C). Taken together, these data further suggest that altered granulopoiesis in *ΔNC16A* mice takes place in bone marrow stromal cells due to loss of BP180 function.

Blocking G-CSF and NF-κB restores normal granulopoiesis in Δ*NC16A* mice

If increased G-CSF is critical for altered granulopoiesis in *ΔNC16A* mice, then blocking G-CSF would restore normal granulocyte level in ΔNC16A mice. To test this hypothesis, anti-G-CSF neutralizing antibody or matched control antibody was administrated i.p. into *ΔNC16A* mice. After 12 days, the granulocyte populations in circulation and bone marrow of the injected mice were analyzed by hematological test and flow cytometry. Granulocyte number in *ΔNC16A* mice treated with G-CSF neutralizing antibody and not matched control antibody were restored to normal levels as shown by hematological test (Figure 6A). Restored granulocyte population frequency was also observed in *ΔNC16A* mice treated with G-CSF neutralizing antibody and not matched control antibody (Figure 6B). To further investigate if the granulocyte-macrophage progenitors (GMPs) were restored to normal level, $Lin^{-}IL\text{-}7R^{-}SCA\text{-}1^{-}c\text{-}kit^{+}CD34^{+}CD16^{+}$ surface marker combination panel were used by flow cytometry. As expected, the granulocyte-macrophage progenitors (GMPs) in anti-G-CSF neutralizing antibody-treated *ΔNC16A* mice were also significantly reduced and close to levels found in WT mice (Figure 6C). These results suggest that G-CSF elevation in bone marrow is a key in myeloid hyperplasia in *ΔNC16A* mice.

G-CSF expression is regulated by NF-κB pathway. Therefore, we tested whether blockading of NF-κB pathway also restores normal level of G-CSF and the granulopoiesis in *ΔNC16A* mice. *ΔNC16A* mice were treated by daily i.p injection of the NF-κB inhibitor pyrolidine dithocarbamate (PDTC, 200mg/kg in PBS) or PBS control for 7 days (54)(55). After 7 days PDTC treatment, activation of NF-κB signaling pathway as evidenced by phosphorylated NF-κB p65 was significantly reduced in bone marrow of PDTC-treated ΔNC16A mice as compared to PBS-treated *ΔNC16A* mice (Figure 6D). G-CSF level (Figure 6E) and granulocyte numbers in circulation (Figure 6F) of PDTC-treated but not control-treated *ΔNC16A* mice were restored to normal level as WT mice. Taken together, these results suggest that NF-κB signaling pathway activation and the subsequently increased G-CSF and granulocytes are the underlying mechanism for altered granulopoiesis in *ΔNC16A* mice.

Discussion

BP180 is well documented as a key cell-cell matrix adhesion molecule in the skin; however, whether it has other biological functions is largely unknown (9). In this study, we generated a new BP180 loss-of-function mouse model (termed *ΔNC16A* mice) by deletion of NC16A domain of humanized NC16A mice (13). Using this model, we demonstrated that loss of BP180 function in bone marrow causes myeloid progenitor lineage skewed toward GMPs,

leading to altered granulopoiesis with significantly increased Gr-1 positive granulocytes in immune organs including bone marrow, spleen, blood and skin. These findings suggest that besides cell-cell matrix adhesion BP180 also plays a role in granulopoiesis.

Abnormal granulopoiesis could arise from cell-autonomous or non-cell-autonomous mechanism. Bone marrow chimera and bone marrow transplantation experiments demonstrated that the granulocyte development in *ΔNC16A* mice is altered in a non-cell autonomous manner. This conclusion is further confirmed by western blotting showing that bone marrow stromal cells and not granulocytes in WT and *ΔNC16A* mice express full-length and truncated BP180, respectively. G-CSF is the most important regulator that drives hematopoiesis stem cells to differentiate into common myeloid progenitors and granulocyte-macrophage progenitors (30). Granulocytes express G-CSF receptor (G-CSFR) (29). Mice lacking G-CSF or G-CSFR show granulopenia (30)(56)(57)(58)(59). We found that increased granulocytes in *ΔNC16A* mice were accompanied with a significantly increased level of G-CSF in bone marrow. Bone marrow MSCs from *ΔNC16A* mice also secreted significantly more G-CSF than WT control mice. Furthermore, treatment with an anti-G-CSF neutralizing antibody restored normal granulopoiesis and normal granulocyte numbers in circulation in *ΔNC16A* mice. Taken together, these findings suggest that lack of BP180 function in MSCs leads to upregulation of G-CSF and subsequently altered granulopoiesis.

Transcription factor NF-κB is critical in regulation of G-CSF and other pro-inflammatory cytokines (43). Mice lacking IκBα have increased granulocyte numbers (44). Cultured human keratinocytes lacking BP180 were reported to secrete inflammatory cytokines associated with activated NF-κB signaling pathway (60). To determine whether activation of the NF-κB pathway is the underlying mechanism in BP180 functional deficiency-caused increased G-CSF and granulocytes, we analyzed the status of NF-κB signaling pathway activation in bone marrow and bone marrow MSCs of *ΔNC16A* mice by Western blot. We found an increased activation of NF-κB signaling pathway in Δ*NC16A* mice as compared to WT control mice. These results suggest that the increased activation of NF-κB signaling pathway and the release of G-CSF in bone marrow MSC contribute to the altered granulopoiesis and subsequently elevated granulocytes in bone marrow, spleen, and peripheral blood. JNK cross-talks with NF-κB pathway and plays an important role in cell survival (61). Phosphorylated JNK is also significantly upregulated in *ΔNC16A* mice (Figure 4F), suggesting potential involvement of JNK in altered granulopoiesis in *ΔNC16A* mice. Future studies are needed to elucidate the role of JNK and functional interaction with NF-κB signaling pathway in the granulopoiesis in *ΔNC16A* mice.

Granulopoiesis could result from intrinsic gene regulation or extrinsic environment cues (21)(62)(63). Periphery infection could lead to unbalanced homeostasis of hematopoietic stem cells, causing emergency granulopoiesis (34). *ΔNC16A* mice develop skin lesions starting at the age of 8 weeks old. This includes reduced skin barrier function that makes *ΔNC16A* mice with skin lesions more prone to infection and development of spontaneous skin inflammation with pruritus; evidence shows infiltration of inflammatory immune cells and an increase of inflammatory cytokines, such as TSLP (46). To rule out the possibility that altered granulopoiesis in 8-week-old or older *ΔNC16A* mice is caused by or partially contributed to by skin lesions/skin inflammation, we determined whether basal keratinocyte-

specific NC16A deletion (termed K14Cre/*ΔNC16A*) also leads to increased granulocytes in immune organs as seen in whole body *ΔNC16A* mice. We found that K14Cre/*ΔNC16A* mice phenocopied skin lesion of *ΔNC16A* mice but had normal granulopoiesis and compatible granulocyte numbers in bone marrow, spleen and blood as WT control mice. To further sustain that skin lesion/skin inflammation is not the main cause for the altered granulopoiesis in *ΔNC16A* mice, we quantified granulocytes in 4-week-old *ΔNC16A* mice when no skin abnormality presents clinically or histologically. Like the 8-week-old *ΔNC16A* mice, 4-week-old *ΔNC16A* mice also exhibited significantly increased granulocytes as compared to WT control. In addition, the NF-kB signaling pathway is also related to TSLP expression by NF-kB binding sites present on the TSLP promoter (64). Furthermore, NF-kB signaling pathway activation leads to secretion of inflammatory cytokines such as TNF-a, Il-1β, IL-13.., which results in increased TSLP expression (65). However, this mechanism needs further investigation in *ΔNC16A* mice. These results suggest that BP180 in bone marrow regulates normal granulopoiesis.

BP180 function loss or dysfunction can be caused by anti-BP180 autoantibodies in BP or BP180 gene mutations in JEB. Our *ΔNC16A* mice reflect more on JEB instead of BP. JEB is a rare genetic disease and present marked skin fragility, blister formation following minor trauma, along with eosinophilia, eosinophils and/or neutrophils infiltrated in the dermis in some cases (14)(17). BP180-functional-deficient mice generated by another group also exhibit a similar skin clinical phenotypes and a significantly increased granulocyte infiltration in the skin (20). However, human patients with JEB have not been reported to have neutrophilia. This discrepancy could be explained by several scenarios: 1) JEB covers a wide spectrum of symptoms among patients, especially due to the BP180 gene mutations (17). Our NC16A truncated mice still have a partially functional BP180 and may reflect a much milder form of JEB (46)(66); 2) JEB is a very rare genetic disease with limited cases reported so far (67). New JEB patients remain to be identified to have a partially functional BP180 and neutrophilia as seen in our NC16A truncated mice; and 3) Human and mice may differ in term of BP180 involvement in granulopoiesis. For example, BP180 regulated granulopoiesis in mice might require other modifier(s) that lack in human. Therefore, our present work provides reverse-genetic evidence linking BP180 function and granulopoiesis. Future clinic studies may support our current findings.

In summary, our results demonstrate for the first time that BP180 as a cell-cell matrix adhesion molecule regulates granulopoiesis. BP180 in bone marrow stromal cells acts on the NF-κB signaling pathway. Loss of BP180 function in these cells leads to increase NF-κB pathway activation and subsequent upregulation of G-CSF and uncontrolled granulopoiesis. Previous reports showed that cultured human and mouse keratinocytes lacking BP180 function secrete inflammatory cytokines associated with activated NF-κB signaling pathway (60)(66). It is of great interest and significance to know if BP180-loss-of-function human marrow MSC behave the same as NC16A-fecifient mouse MSC and if BP180 regulates NF-kB pathway in other cell lineages besides MSC and keratinocytes. Our future studies will directly address these issues by using gene editing to determine the role of BP180 in the signaling pathways of human cells. Our findings point to new directions for increased understanding of the pathophysiology of diseases associated with BP180 loss-of-function and abnormal granulopoiesis. However, it remains unclear whether BP180 plays a different

role at different stages of granulocyte development and how BP180 regulates NF-κB pathway at the molecular level.

Supplementary Material

Refer to Web version on PubMed Central for supplementary material.

Acknowledgments and author's contribution.

L.L., BJ.H., N.L., and Z.L. designed the study; L.L., BJ.H., P.G., and Z.L. conducted experiments; L.L., BJ.H., N.L., E.M., B.V., J.T., and Z.L. analyzed data; L.A.D. provided reagents; and L.L., BJ.H., P.G., E.M., B.V., N.E.T., J.T., and Z.L. wrote the manuscript. The authors thank Dr. Dennis Roop at the University of Colorado at Denver for providing K14Cre mice.

Financial support:

This work was supported by the NIH (R01 AI40768 and R01 AI61430 to Z. Liu), the UNC Cancer Center Research Award (to Z. Liu), UNC Graduate School Dissertation Completion Fellowship (to L. Lin) and P01CA206980 to N. Thomas.

References

1. Hammers CM, and Stanley JR. 2016 Mechanisms of Disease: Pemphigus and Bullous Pemphigoid. Annu. Rev. Pathol. Mech. Dis 11: 175–197.
2. Koster J, Geerts D, Favre B, Borradori L, and Sonnenberg A. 2003 Analysis of the interactions between BP180, BP230, plectin and the integrin alpha6beta4 important for hemidesmosome assembly. J. Cell Sci 116: 387–399. [PubMed: 12482924]
3. Hopkinson SB, and Jones JC. 2000 The N terminus of the transmembrane protein BP180 interacts with the N-terminal domain of BP230, thereby mediating keratin cytoskeleton anchorage to the cell surface at the site of the hemidesmosome. Mol Biol Cell 11: 277–286. [PubMed: 10637308]
4. Margadant C, Frijns E, Wilhelmsen K, and Sonnenberg A. 2008 Regulation of hemidesmosome disassembly by growth factor receptors. Curr. Opin. Cell Biol 20: 589–596. [PubMed: 18583123]
5. Diaz LA, Ratrie H, Saunders WS, Futamura S, Squiquera HL, Anhalt GJ, and Giudice GJ. 1990 Isolation of a human epidermal cDNA corresponding to the 180-kD autoantigen recognized by bullous pemphigoid and herpes gestationis sera: Immunolocalization of this protein to the hemidesmosome. J. Clin. Invest 86: 1088–1094. [PubMed: 1698819]
6. Liu Z, Diaz L. a., Troy JL, Taylor AF, Emery DJ, Fairley J. a., and Giudice GJ. 1993 A passive transfer model of the organ-specific autoimmune disease, bullous pemphigoid, using antibodies generated against the hemidesmosomal antigen, BP180. J. Clin. Invest 92: 2480–2488. [PubMed: 7693763]
7. Foldes C, Wallach D, Aubiniere E, Vignon-Pennamen MD, and Cottenot F. 1988 Generalized atrophic benign form of junctional epidermolysis bullosa. Dermatologica 176: 83–90. [PubMed: 2453379]
8. Darling TN, Bauer JW, Hintner H, and Yancey KB. 1997 Generalized atrophic benign epidermolysis bullosa. Adv. Dermatol 13: 87–119; discussion 120. [PubMed: 9551142]
9. Leighty L, Li N, Diaz LA, and Liu Z. 2007 Experimental models for the autoimmune and inflammatory blistering disease, Bullous pemphigoid. Arch. Dermatol. Res 299: 417–422. [PubMed: 17879094]
10. Nousari HC, and Anhalt GJ. 1999 Pemphigus and bullous pemphigoid. Lancet 354: 667–672. [PubMed: 10466686]
11. Giudice GJ, Emery DJ, Zelickson BD, Anhalt GJ, Liu Z, and a Diaz L. 1993 Bullous pemphigoid and herpes gestationis autoantibodies recognize a common non-collagenous site on the BP180 ectodomain. J. Immunol 151: 5742–5750. [PubMed: 8228259]

12. Zillikens D, Rose PA, Balding SD, Liu Z, Olague-Marchan M, Diaz LA, and Giudice GJ. 1997 Tight clustering of extracellular BP180 epitopes recognized by bullous pemphigoid autoantibodies. J. Invest. Dermatol 109: 573–9. [PubMed: 9326393]
13. Liu Z, Sui W, Zhao M, Li Z, Li N, Thresher R, Giudice GJ, Fairley JA, Sitaru C, Zillikens D, Ning G, Marinkovich MP, and Diaz LA. 2008 Subepidermal blistering induced by human autoantibodies to BP180 requires innate immune players in a humanized bullous pemphigoid mouse model. J. Autoimmun 31: 331–338. [PubMed: 18922680]
14. Bruckner-Tuderman L, McGrath JA, Robinson EC, and Uitto J. 2013 Progress in Epidermolysis bullosa research: summary of DEBRA International Research Conference 2012. J Invest Dermatol 133: 2121–2126. [PubMed: 23949764]
15. Jonkman MF, de Jong MC, Heeres K, Pas HH, van der Meer JB, Owaribe K, Martinez de Velasco AM, Niessen CM, and Sonnenberg A. 1995 180-kD bullous pemphigoid antigen (BP180) is deficient in generalized atrophic benign epidermolysis bullosa. J. Clin. Invest 95: 1345–1352. [PubMed: 7883981]
16. Yuen WY, Pas HH, Sinke RJ, and Jonkman MF. 2011 Junctional epidermolysis bullosa of late onset explained by mutations in COL17A1. Br. J. Dermatol 164: 1280–4. [PubMed: 21466533]
17. Kiritsi D, Kern JS, Schumann H, Kohlhase J, Has C, and Bruckner-Tuderman L. 2011 Molecular mechanisms of phenotypic variability in junctional epidermolysis bullosa. J. Med. Genet 48: 450–457. [PubMed: 21357940]
18. Mabuchi E, Umegaki N, Murota H, Nakamura T, Tamai K, and Katayama I. 2007 Oral steroid improves bullous pemphigoid-like clinical manifestations in non-Herlitz junctional epidermolysis bullosa with COL17A1 mutation. Br. J. Dermatol 157: 596–598. [PubMed: 17596158]
19. Cifuentes L, Kiritsi D, Chen W, Pennino J, Ring J, Weidinger S, and Has C. 2013 A case of junctional epidermolysis bullosa with prurigo-like lesions and reduction of collagen XVII and filaggrin. Br. J. Dermatol 169: 195–198. [PubMed: 23834121]
20. Hurskainen T, Kokkonen N, Sormunen R, Jackow J, Löffek S, Soininen R, Franzke C-W, Bruckner-Tuderman L, and Tasanen K. 2015 Deletion of the Major Bullous Pemphigoid Epitope Region of Collagen XVII Induces Blistering, Autoimmunization, and Itching in Mice. J. Invest. Dermatol 135: 1303–1310. [PubMed: 25310407]
21. Friedman AD 2007 Transcriptional control of granulocyte and monocyte development. Oncogene 26: 6816–6828. [PubMed: 17934488]
22. Eaves C 2015 Hematopoietic stem cells: concepts, definitions, and the new reality. Blood 125: 2605–2614. [PubMed: 25762175]
23. Gottgens B 2015 Regulatory network control of blood stem cells. Blood 125: 2614–2621. [PubMed: 25762179]
24. Boulais P, and Frenette P. 2015 Making sense of hematopoietic stem cell niches. Blood 125: 2621–2630. [PubMed: 25762174]
25. Amulic B, Cazalet C, Hayes GL, Metzler KD, and Zychlinsky A. 2012 Neutrophil Function : From Mechanisms to Disease. Annu. Rev. Immunol 30: 459–489. [PubMed: 22224774]
26. Nauseef WM, and Borregaard N. 2014 Neutrophils at work. Nat. Reveiw Immunol 15: 602–611.
27. Panopoulos AD, and Watowich SS. 2008 Cytokine Granulocyte colony-stimulating factor : Molecular mechanisms of action during steady state and ‘ emergency ‘ hematopoiesis. Cytokine 42: 277–288. [PubMed: 18400509]
28. Yoda M, Kimura T, Tohmonda T, Uchikawa S, Koba T, Takito J, Morioka H, Matsumoto M, Link DC, Chiba K, Okada Y, Toyama Y, and Horiuchi K. 2011 Dual functions of cell-autonomous and non-cell-autonomous ADAM10 activity in granulopoiesis. Blood 118: 6939–42. [PubMed: 22042698]
29. Beekman R, and Touw IP. 2010 G-CSF and its receptor in myeloid malignancy. Blood 115: 5131–5137. [PubMed: 20237318]
30. Basu S, Dunn A, and Ward A. 2002 G-CSF: function and modes of action (Review). Int. J. Mol. Med 10: 3–10. [PubMed: 12060844]
31. Bajrami B, Zhu H, Kwak HJ, Mondal S, Hou Q, Geng G, Karatepe K, Zhang YC, Arrieta CN, Park SY, Loison F, Sakai J, Xu Y, Silberstein LE, and Luo HR. 2016 G-CSF maintains controlled

neutrophil mobilization during acute inflammation by negatively regulating CXCR2 signaling. J. Exp. Med 213: 1999–2018. [PubMed: 27551153]

32. Boettcher S, Gerosa RC, Radpour R, Bauer J, Ampenberger F, Heikenwalder M, Kopf M, and Manz MG. 2014 Endothelial cells translate pathogen signals into G-CSF – driven emergency granulopoiesis. Blood 124: 1393–1404. [PubMed: 24990886]
33. Tomicic M, Starcevic M, Zach V, Bingulac-popovic J, and Hundric-haspl Z. 2009 Case Report A Case of Neonatal Neutropenia Due to Anti-Fc Gamma Receptor IIIb Isoantibodies Treated with Recombinant Human Granulocyte Colony Stimulating Factor. Case Rep. Med Article ID 717545.
34. Manz MG, and Boettcher S. 2014 Emergency granulopoiesis. Nat. Reveiws Immunol 14: 302–314.
35. Akala OO, and Clarke MF. 2006 Hematopoietic stem cell self-renewal. Curr. Opin. Genet. Dev 16: 496–501. [PubMed: 16919448]
36. Pajcini KV, Speck NA, and Pear WS. 2011 Notch signaling in mammalian hematopoietic stem cells. Leukemia 25: 1525–1532. [PubMed: 21647159]
37. Yao D, Huang Y, Huang X, Wang W, Yan Q, Wei L, Xin W, Gerson S, Stanley P, Lowe JB, and Zhou L. 2017 Protein O -fucosyltransferase 1 (Pofut1) regulates lymphoid and myeloid homeostasis through modulation of Notch receptor ligand interactions. Blood 117: 5652–5663.
38. Khalaj M, and Park CY. 2014 Previews Notch One Up to Stroma : Endothelial Notch Prevents Inflammation and Myeloproliferation. Stem Cell 15: 1–2.
39. Calvi LM, and Link DC. 2015 Perspectives The hematopoietic stem cell niche in homeostasis and disease. Blood 126: 2443–2451. [PubMed: 26468230]
40. Wang L, Zhang H, Rodriguez S, Cao L, Parish J, Mumaw C, Zollman A, Kamoka MM, Mu J, Chen DZ, Srour EF, Chitteti BR, HogenEsch H, Tu X, Bellido TM, Boswell HS, Manshouri T, Verstovsek S, Yoder MC, Kapur R, Cardoso AA, and Carlesso N. 2014 Notch-dependent repression of miR-155 in the bone marrow niche regulates hematopoiesis in an NF-??B-dependent manner. Cell Stem Cell 15: 51–65. [PubMed: 24996169]
41. Zhao C, Xiu Y, Ashton J, Xing L, Morita Y, Jordan CT, and Boyce BF. 2012 Noncanonical NF-KB signaling regulates hematopoietic stem cell self-renewal and microenvironment interactions. Stem Cells 30: 709–718. [PubMed: 22290873]
42. Napetschnig J, and Wu H. 2013 Molecular basis of NF-κB signaling. Annu. Rev. Biophys 42: 443–68. [PubMed: 23495970]
43. Grigoriadis G, Zhan Y, Grumont RJ, Metcalf D, Handman E, Cheers C, and Gerondakisl S. 1996 The Rel subunit of NF-kB-like transcription factors is a positive and negative regulator of macrophage gene expression : distinct roles for Rel in different macrophage populations. EMBO J. 15: 7099–7107. [PubMed: 9003785]
44. Beg A, Sha W, Bronston R, and Baltimore D. 1995 Constitutive NF-KB activation, enhanced granulopoiesis, and neonatal lethality in IKBa-deficient mice. Gene Dev. 9: 2736–2746. [PubMed: 7590249]
45. Mankan AK, Canli O, Schwitalla S, Ziegler P, Tschopp J, Korn T, and Greten FR. 2011 TNF- α – dependent loss of IKK β -deficient myeloid progenitors triggers a cytokine loop culminating in granulocytosis. Proc. Natl. Acad. Sci. U. S. A 108: 6567–6572. [PubMed: 21464320]
46. Zhang Y, Hwang B-J, Liu Z, Li N, Lough K, Williams SE, Chen J, Burette SW, Diaz LA, Su MA, Xiao S, and Liu Z. 2018 BP180 dysfunction triggers spontaneous skin inflammation in mice. Proc. Natl. Acad. Sci 115: 6434–6439. [PubMed: 29866844]
47. Spangrude GJ 2008 Assessment of Lymphocyte Development in Radiation Bone Marrow Chimeras. Curr. Protoc. Immunol 4.61–4.6.9. [PubMed: 18729062]
48. Maryanovich M, and Gross A. 2014 Competitive Bone Marrow Transplantation. Bio-protocol 4: e1145.
49. Petit I, Szyper-kravitz M, Nagler A, Lahav M, Peled A, Habler L, Ponomaryov T, Taichman RS, Arenzana-seisdedos F, Fujii N, Sandbank J, Zipori D, and Lapidot T. 2002 G-CSF induces stem cell mobilization by decreasing bone marrow SDF-1 and up-regulating CXCR4. Nat. Immunol 3: 687–694. [PubMed: 12068293]
50. Soleimani M, and Nadri S. 2009 A protocol for isolation and culture of mesenchymal stem cells from mouse bone marrow. Nat. Protoc 4: 102–106. [PubMed: 19131962]

51. Kawakatsu M, Urata Y, Goto S, Ono Y, and Li T. 2013 Placental extract protects bone marrow-derived stem / progenitor cells against radiation injury through anti-inflammatory activity. J. Radiat. Res 54: 268–276. [PubMed: 23154884]
52. Wilson A, and Trumpp A. 2006 Bone-marrow haematopoietic-stem-cell niches. Nat. Rev. Immunol 6: 93–106. [PubMed: 16491134]
53. Hoggatt J, Kfoury Y, and Scadden DT. 2016 Hematopoietic Stem Cell Niche in Health and Disease. Annu. Rev. Pathol. Mech. Dis 11: 555–581.
54. Schreck B, Meier B, Daniela NM, Drge W, and Baeuerle PA. 1992 Dithiocarbamates as Potent Inhibitors of Nuclear Factor KB Activation in Intact Cells. J. Exp. Med 175: 1181–1194. [PubMed: 1314883]
55. Liu SF, Ye X, and Malik AB. 1999 Inhibition of NF-kB Activation by Pyrrolidine Dithiocarbamate Prevents In Vivo Expression of proinflammatory genes. Circulation 100: 1330–7. [PubMed: 10491379]
56. Lieschke BGJ, Grail D, Hodgson G, Metcalf D, Stanley E, Cheers C, Fowler KJ, Basu S, Zhan YF, and Dunn AR. 1994 Mice Lacking Granulocyte Colony-Stimulating Factor Have Chronic Neutropenia, Granulocyte and Macrophage Progenitor Cell Deficiency, and Impaired Neutrophil Mobilization. Blood 84: 1737–1747. [PubMed: 7521686]
57. Liu F, Wu HY, Wesselschmidt R, Kornaga T, and Link DC. 1996 Impaired Production and Increased Apoptosis of Neutrophils in Granulocyte Colony-Stimulating Factor Receptor – Deficient Mice. Immunity 5: 491–501. [PubMed: 8934575]
58. Roberts AW 2005 G-CSF : A key regulator of neutrophil production, but that is not all ! Growth Factor 23: 33–41.
59. Basu S, Hodgson G, Katz M, and Dunn AR. 2002 Evaluation of role of G-CSF in the production, survival, and release of neutrophils from bone marrow into circulation. Blood 100: 854–862. [PubMed: 12130495]
60. Van den Bergh F, Eliason SL, Burmeister BT, and Giudice GJ. 2012 Collagen XVII (BP180) modulates keratinocyte expression of the proinflammatory chemokine, IL-8. Exp. Dermatol 21: 605–611. [PubMed: 22775995]
61. Nakano H 2004 Signaling crosstalk between NF-kB and JNK. Trends Immunol. 25: 402–405. [PubMed: 15275637]
62. Strydom N, and Rankin SM. 2013 Regulation of Circulating Neutrophil Numbers under Homeostasis and in Disease. J. Innate Immun 5: 304–314. [PubMed: 23571274]
63. Christopher MJ, and Link DC. 2007 Regulation of neutrophil homeostasis. Curr. Opin. Hematol 14: 3–8. [PubMed: 17133093]
64. Cultrone A, de Wouters T, Lakhdari O, Kelly D, Mulder I, Logan E, Lapaque N, Doré J, and Blottière HM. 2013 The NF-κB binding site located in the proximal region of the TSLP promoter is critical for TSLP modulation in human intestinal epithelial cells. Eur. J. Immunol 43: 1053–1062. [PubMed: 23310954]
65. Redhu NS, Saleh A, Halayko AJ, Ali AS, and Gounni AS. 2011 Essential role of NF-kB and AP-1 transcription factors in TNF-α-induced TSLP expression in human airway smooth muscle cells. Am. J. Physiol. - Lung Cell. Mol. Physiol 300: 479–485.
66. Hwang BJ, Zhang Y, Brozowski JM, Liu Z, Burette S, Lough K, Smith CC, Shan Y, Chen J, Li N, Williams S, Su M, Googe P, Thomas NE, and Liu Z. 2019 The dysfunction of BP180/collagen XVII in keratinocytes promotes melanoma progression. Oncogene 38: 7491–7503. [PubMed: 31435021]
67. Fine J-D 2010 Inherited Epidermolysis Bullosa. Orphanet J. Rare Dis 5: 561–568.

Key points:

- BP180 is expressed in bone marrow mesenchymal stem cells.
- BP180 in bone marrow mesenchymal stem cells regulates granulopoiesis.

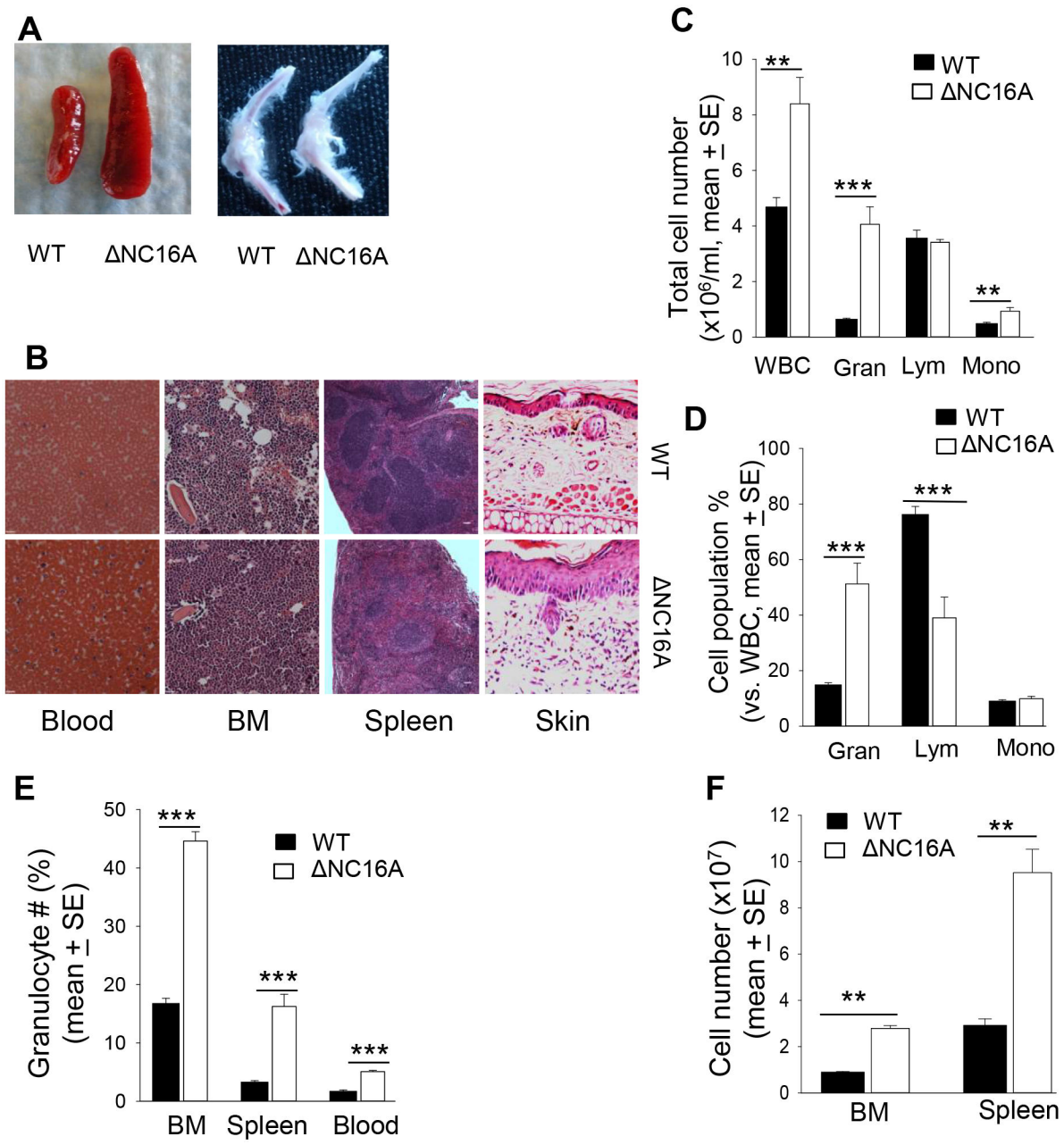

Figure 1. Granulocyte hyperplasia in Δ*NC16A* mice.

(A) Biopsy examination of spleen and bone. Representatives of gross anatomy of spleen and bone marrow of WT and *ΔNC16A* mice. Splenomegaly was observed in *ΔNC16A* mice at age of 8–12 weeks, and the bone of *ΔNC16A* mice was less red than WT mice. (B) Granulocyte infiltration. H/E staining showed increased granulocytes in blood, increased cellularity in bone marrow (BM), increased red pulp in spleen, and increased infiltrating granulocytes in dermis of *ΔNC16A* mice compared to WT mice. (C) Hematological examination. Complete blood count showed significantly increased white blood cells, granulocytes and monocytes in peripheral blood of *ΔNC16A* mice compared to WT mice (n=8, **p<0.01, ***p<0.001). WBC, white blood cell; Lym, lymphocyte; Mono, monocyte.

(D) Relative cell population. Percentage of granulocyte populations was also increased significantly, while lymphocyte population was significantly decreased in peripheral blood of *ΔNC16A* mice compared to WT mice (n=8, ***p<0.001). (E) Granulocyte cell frequency. Granulocytes in bone marrow, spleen and blood of WT and *ΔNC16A* mice were analyzed by flow cytometry using forward scatter (cell size) and side scatter (granularity). Granulocyte populations in these three immune sites were around 3 folds increased in *ΔNC16A* mice than WT mice, and the increase was statistically significant (n=6, ***p<0.001). (F) Granulocyte cell number. Neutrophil numbers were quantified by flow cytometry using neutrophil specific surface markers CD11b and Gr-1. Neutrophils were significantly increased in *ΔNC16A* mice than WT mice, and the difference is statistically significant (n=6, **p<0.01).

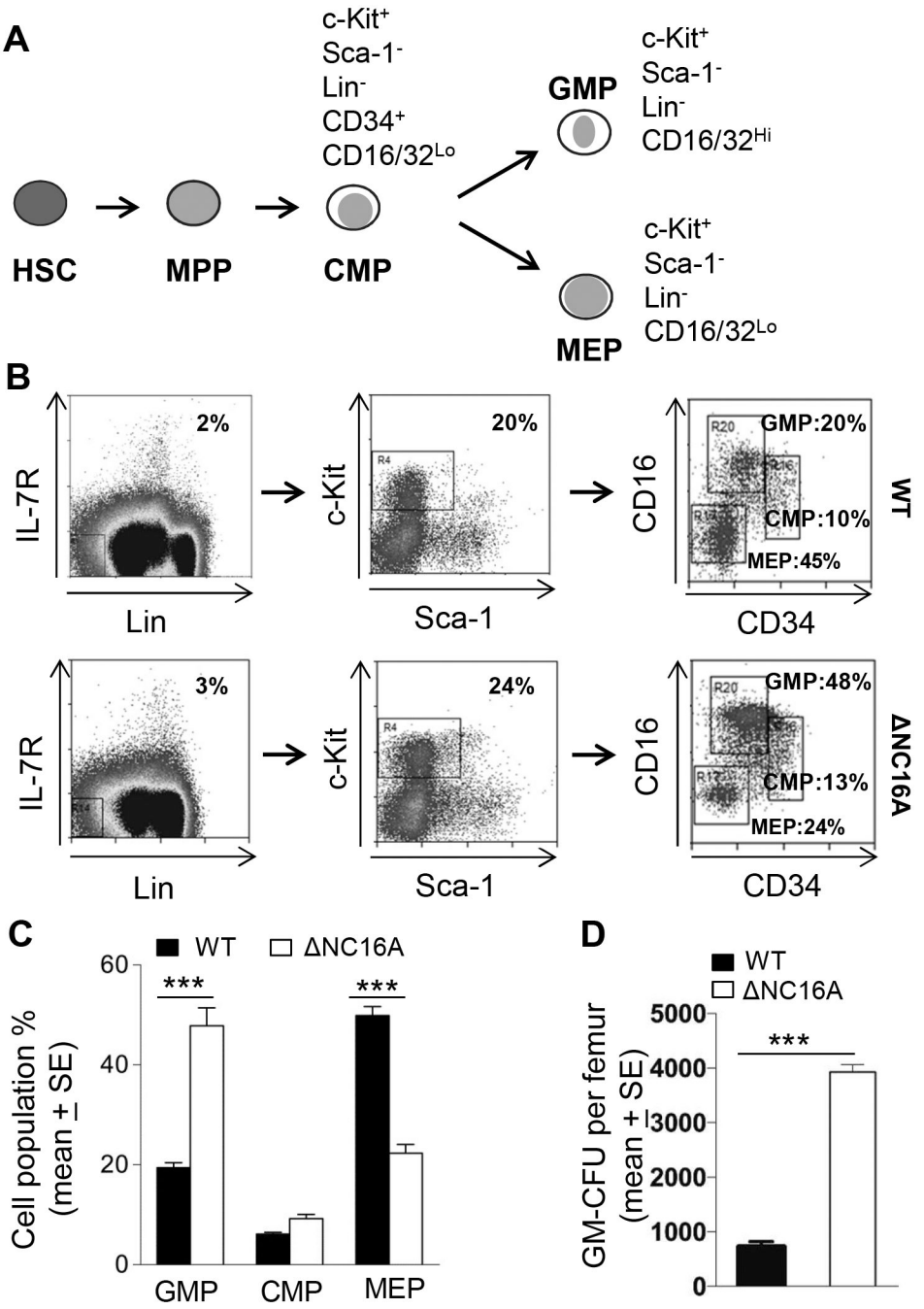

Figure 2. Increased granulocyte-monocyte progenitor in Δ*NC16A* mice.

(A) Diagram showing different stages of granulopoiesis and surface markers expressed in different developmental stages. HSC, hematopoietic stem cell; MMP, multipotent progenitor; CMP, common myeloid progenitor; GMP, granulocyte-monocyte progenitor; MEP, megakaryocyte-erthrocyte progenitor. (B) Flow cytometry. Bone marrow cells were gated on Lin and IL-7R double negative cells, and c-Kit positive and Sca-1 negative cell population was used for further analysis. CD34 and CD16 were stained to distinguish GMP, CMP and MEP. Using $Lin^{-}Sca\text{-}1^{-}$ $c\text{-}Kit^{+}CD34^{+}$ $CD16^{lo}$ panel as common myeloid

progenitor (CMP) population markers and Lin^{-} $Sca\text{-}1^{-}$ $c\text{-}Kit^{+}$ $CD16^{hi}$ as granulocyte-monocyte progenitor(GMP) markers, GMP were more than 2 folds increased in bone marrow of *ΔNC16A* mice than WT. (C) Statistical analysis showed significantly increased GMP in bone marrow of *ΔNC16A* mice than WT, in contrast MEP were decreased in *ΔNC16A* mice than WT (n=6, ***p<0.001). (D) Bone marrow cells were cultured by methycellulose-based media, colonies were counted after 12 days culture. *ΔNC16A* mice have more granulocyte/monocyte colony-forming units (GM-CFU) than WT mice (n=6, ***p<0.001).

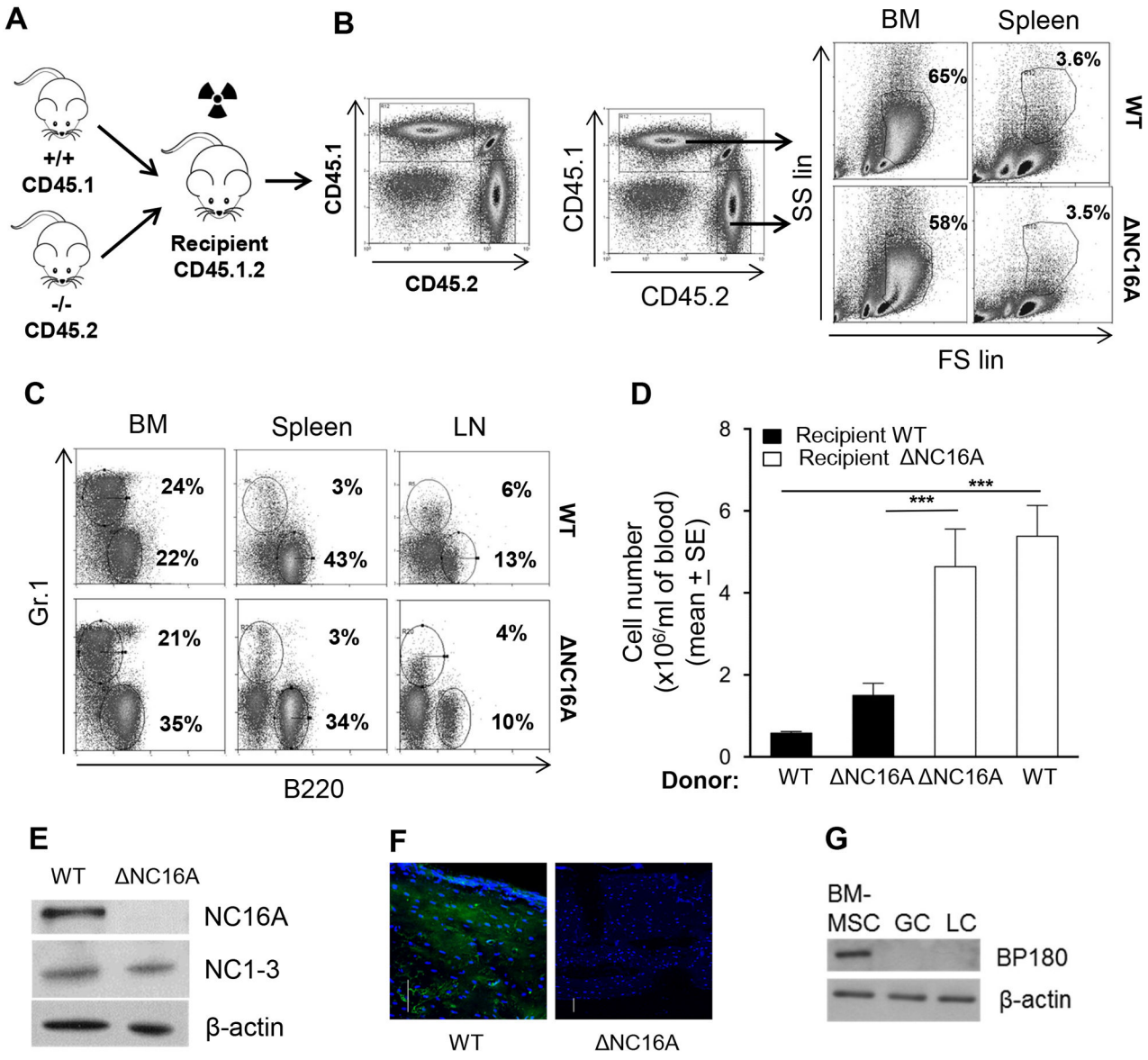

Figure 3. Granulocyte hyperplasia in Δ*NC16A* mice were caused by extrinsic factors.

(A) Diagram of bone marrow chimera experiment. Bone marrows from WT CD45.1 and *ΔNC16A* CD45.2 mice were mixed by 1:1 ratio and were transferred to sublethally irradiated(700cGy) recipient CD45.1.2 mice by i.v. Eight weeks post reconstitution, surface markers were used for determining different populations of cells by flow cytometry. Granulocyte populations from WT and *ΔNC16A* mice in bone marrow and spleen were comparable tested by forward scatter (cell size) and side scatter (granularity) (B) and by using granulocytes specific marker Gr-1+ (C). (D) Reciprocal transplantation experiment. WT CD45.1 bone marrow was transferred to sublethally irradiated (700cGy) recipient *ΔNC16A* CD45.2 mice, while *ΔNC16A* CD45.2 bone marrow was transferred to WT CD45.1 sublethally irradiated (700cGy) recipient mice. Total blood granulocytes were counted by hematological examination 8 weeks post bone marrow transplantation (50ul of blood were used for counting). WT recipients receiving bone marrow cells either from WT

or *ΔNC16A* mice had normal granulocyte numbers, while *ΔNC16A* recipients receiving bone marrow cells either from WT or *ΔNC16A* mice exhibited significantly higher number of granulocytes (n=6, ***p<0.001). (E) Immunoblotting showed full-length BP180 in WT bone marrow and NC16A truncated BP180 in *ΔNC16A* bone marrow. (F) Indirect immunofluorescence exhibited anti-NC16A antibody staining in WT and not *ΔNC16A* bone marrow. (G) Immunoblotting identified BP180 in MSC and not granulocytes (GC) and lymphocytes (LC).

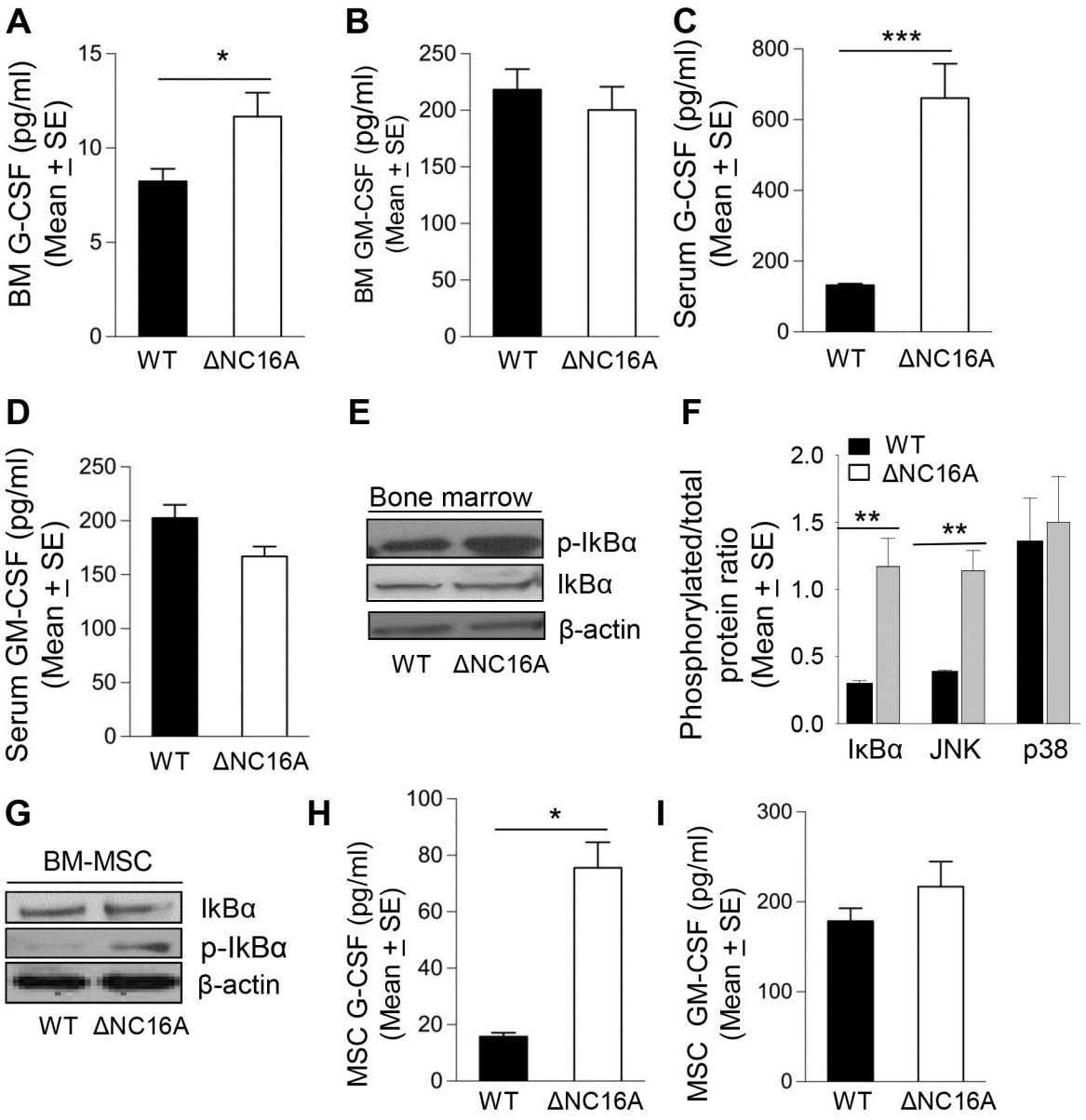

Figure 4. Δ*NC16A* mice showed elevated G-CSF level and increased activation of NF-κB signaling pathway in bone marrow.

ELISA assays revealed significantly elevated levels of G-CSF in bone marrow (A) and blood (B) of *ΔNC16A* mice as compared to WT control, whereas levels of GM-CSF in bone marrow (C) and blood (D) of both WT and *ΔNC16A* mice were compatible (n=8, *p<0.05, ***p<0.001). (E) Protein extracts made from total bone marrow cells (whole bone marrow flush) of WT and *ΔNC16A* mice were analyzed by immunoblotting. Higher levels of phospho-IκBα were seen in *ΔNC16A* mice than in WT mice. (F) Phosphorylated IκBα and JNK were significantly increased in bone marrow of *ΔNC16A* mice than in WT mice as determined by densitometry analysis of the phosphorylated vs. total signaling proteins (n=4, **p<0.01). (G) Bone marrow-derived mesenchymal stem cells (MSC) from *ΔNC16A* mice showed increased activation of NF-κB pathway. (H) ELISA assay of MSC culture medium revealed significantly higher levels of G-CSF in bone marrow derived MSC of *ΔNC16A*

mice as compared to WT control (n=6, ***p<0.001). (I) Levels of bone marrow derived MSC-released GM-CSF were similar between WT and *ΔNC16A* mice.

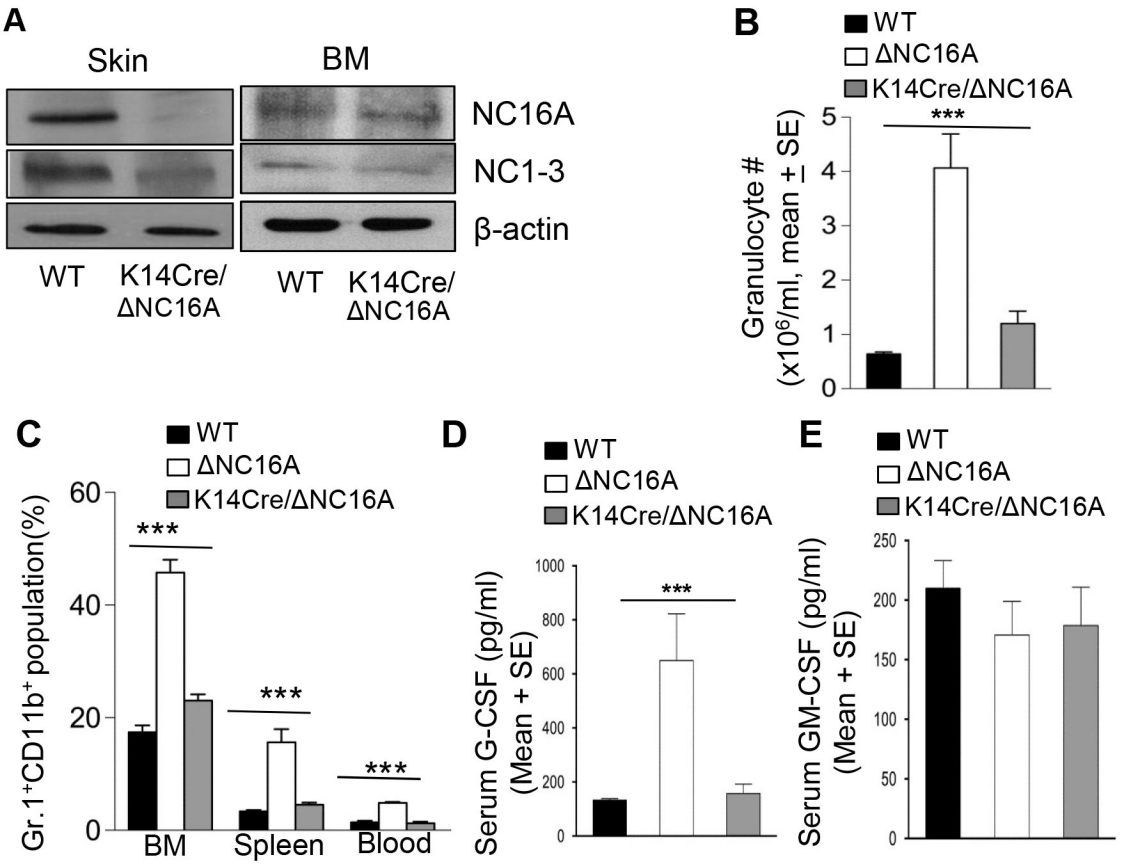

Figure 5. K14Cre/Δ*NC16A* mice had normal granulopoiesis.

(A) Immunoblotting confirmed that keratinocyte-specific *ΔNC16A* (K14Cre/*ΔNC16A*) mice express NC16A truncated BP180 in the skin and full-length BP180 in bone marrow. (B) Hematological examination showed that K14Cre/*ΔNC16A* mice had significantly lower periphery granulocytes compared to *ΔNC16A* mice (n=6, ***p<0.001), which is similar to WT. (C) By flow cytometry for Gr.1 and CD11b double positive cell, K14Cre/*ΔNC16A* and WT mice had compatible granulocyte populations in bone marrow, spleen and blood, which are significantly lower than $Gr1^{+}CD11b^{+}$ cells in *ΔNC16A* mice (n=6, ***p<0.001). ELISA assays also revealed similar levels of serum G-CSF (D) and GM-CSF (E) between K14Cre/*ΔNC16A* and WT mice (n=6, ***p<0.001, K14Cre/*ΔNC16A* vs. *ΔNC16A*).

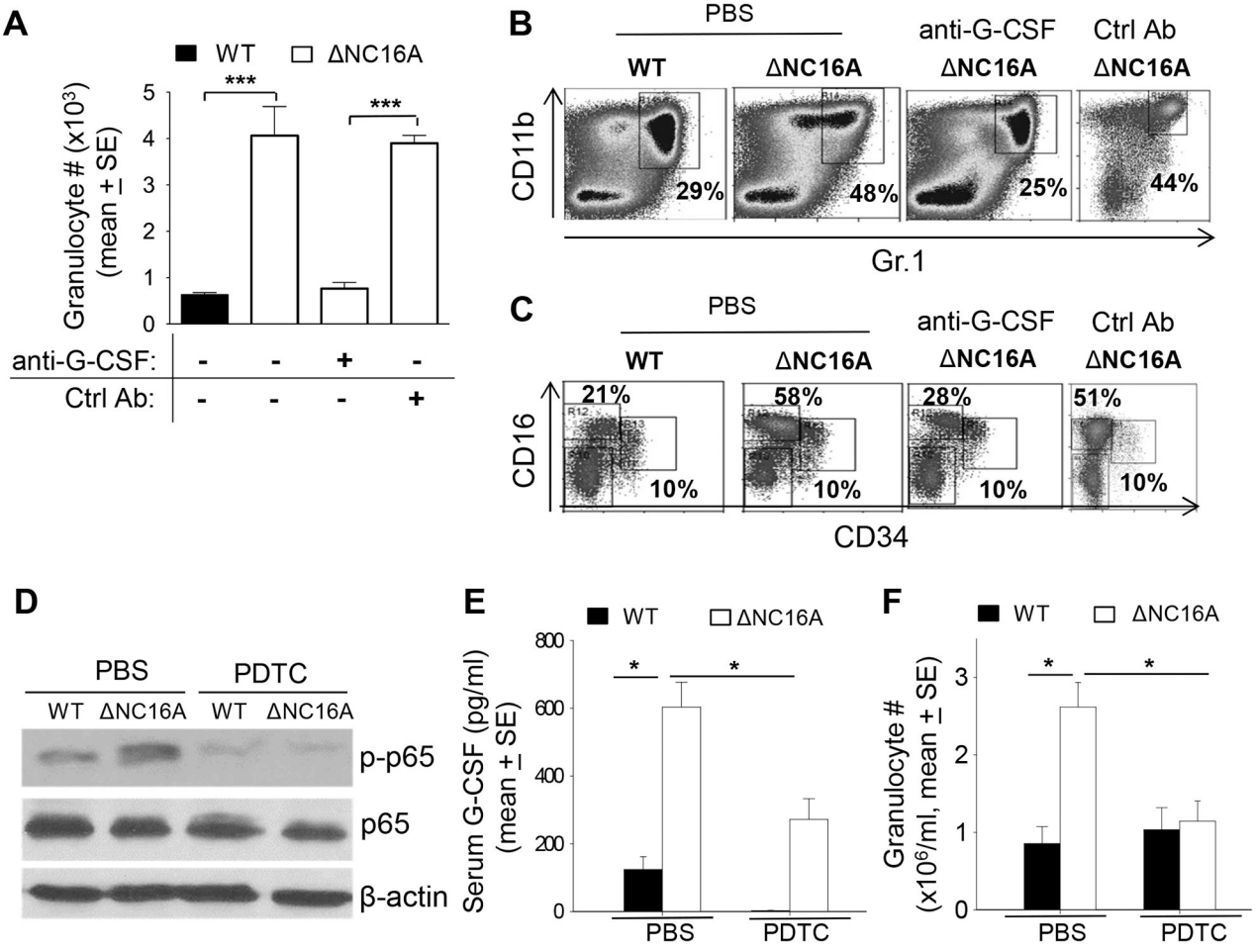

Figure 6. Blocking G-CSF and NF-κB restored normal granulopoiesis in Δ*NC16A* mice.

WT and *ΔNC16A* mice were i.p. treated with anti-G-CSF neutralizing antibody or matched control antibody. PBS-treated WT and *ΔNC16A* mice were also included as control. Granulocytes and granulocyte monocyte progenitor (GMP) were analyzed by hematological examination and flow cytometry at day 12 post treatment. (A) Complete cell count. Hematological test showed that anti-G-CSF antibody and not control antibody treatment reduced granulocyte population in *ΔNC16A* mice down to level similar to WT mice (n=6. ***p<0.001). (B) Flow cytometry using CD11b and Gr.1 surface markers showed that anti-G-CSF neutralizing antibody and not control antibody treatment restored granulocyte level in *ΔNC16A* mice comparable to WT control mice. (C) Flow cytometry using Lin, Sca-1, c-Kit CD16 and CD34 markers showed that GMP level in bone marrow of *ΔNC16A* mice was also restored to the level of WT control 12 days after anti-G-CSF antibody and not control antibody treatment. (D) WT and *ΔNC16A* mice were i.p injected daily for 7 days with PDTC or PBS vehicle control. (A) Western blotting showed that PDTC significantly reduced NF-κB activation (p65 phosphorylation) in bone marrow cells of *ΔNC16A* mice. (E) ELISA assay showed that PDTC treated *ΔNC16A* mice had serum G-CSF similar to WT control. (F) Hematological test showed that granulocyte level of PDTC treated *ΔNC16A* mice reduced to a similar level as WT mice (n=6, * p<0.05).